

Statistics of the MLE and Approximate Upper and Lower Bounds – Part 1: Application to TOA Estimation

Achraf Mallat, *Member, IEEE*, Sinan Gezici, *Senior Member, IEEE*, Davide Dardari, *Senior Member, IEEE*,
Christophe Craeye, *Member, IEEE*, and Luc Vandendorpe, *Fellow, IEEE*

Abstract—In nonlinear deterministic parameter estimation, the maximum likelihood estimator (MLE) is unable to attain the Cramer-Rao lower bound at low and medium signal-to-noise ratios (SNR) due the threshold and ambiguity phenomena. In order to evaluate the achieved mean-squared-error (MSE) at those SNR levels, we propose new MSE approximations (MSEA) and an approximate upper bound by using the method of interval estimation (MIE). The mean and the distribution of the MLE are approximated as well. The MIE consists in splitting the *a priori* domain of the unknown parameter into intervals and computing the statistics of the estimator in each interval. Also, we derive an approximate lower bound (ALB) based on the Taylor series expansion of noise and an ALB family by employing the binary detection principle. The accurateness of the proposed MSEAs and the tightness of the derived approximate bounds¹ are validated by considering the example of time-of-arrival estimation.

Index Terms—Nonlinear estimation, threshold and ambiguity phenomena, maximum likelihood estimator, mean-squared-error, upper and lower bounds, time-of-arrival.

I. INTRODUCTION

NONLINEAR estimation of deterministic parameters suffers from the threshold effect [2–11]. This effect means that for a signal-to-noise ratio (SNR) above a given threshold, estimation can achieve the Cramer-Rao lower bound (CRLB), whereas for SNRs lower than that threshold, estimation deteriorates drastically until the estimate becomes uniformly distributed in the *a priori* domain of the unknown parameter.

As depicted in Fig. 1(a), the SNR axis can be split into three regions according to the achieved mean-squared-error (MSE):

- 1) *A priori* region: Region in which the estimate is uniformly distributed in the *a priori* domain of the unknown parameter (region of low SNRs).
- 2) Threshold region: Region of transition between the *a priori* and asymptotic regions (region of medium SNRs).

Achraf Mallat, Christophe Craeye and Luc Vandendorpe are with the ICTEAM Institute, Université Catholique de Louvain, Belgium. Email: {Achraf.Mallat, Christophe.Craeye, Luc.Vandendorpe}@uclouvain.be.

Sinan Gezici is with the Department of Electrical and Electronics Engineering, Bilkent University, Ankara 06800, Turkey. Email: gezici@ee.bilkent.edu.tr.

Davide Dardari is with DEI, CNIT at University of Bologna, Italy. Email: davide.dardari@unibo.it.

This work has been supported in part by the Belgian network IAP Bestcom and the EU network of excellence NEWCOM#.

¹The derived magnitudes are referred as “bounds” because they are either lower or greater than the MSE, and as “approximate” because an approximation is performed to obtain them; the terminology “approximate bound” was previously used by McAulay in [1].

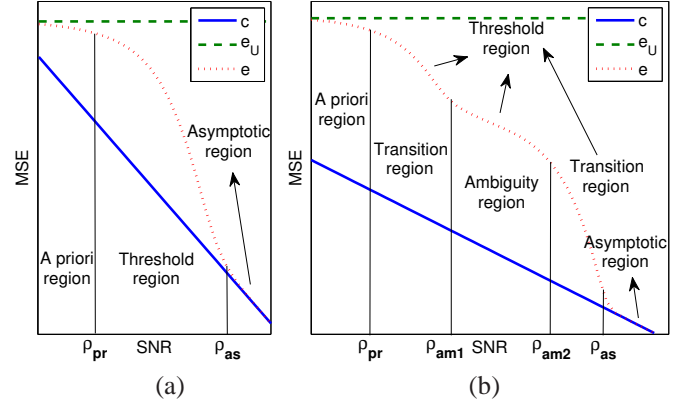


Figure 1. SNR regions (a) *A priori*, threshold and asymptotic regions for non-oscillating ACRs (b) *A priori*, ambiguity and asymptotic regions for oscillating ACRs (c: CRLB, e_U : MSE of uniform distribution in the *a priori* domain, e : achievable MSE, ρ_{pr} , ρ_{am1} , ρ_{am2} , ρ_{as} : *a priori*, begin-ambiguity, end-ambiguity and asymptotic thresholds).

- 3) Asymptotic region: Region in which the CRLB is achieved (region of high SNRs).

In addition, if the autocorrelation (ACR) of the signal carrying the information about the unknown parameter is oscillating, then estimation will be affected by the ambiguity phenomenon [12, pp. 119] and a new region will appear so the SNR axis can be split, as shown Fig. 1(b), into five regions:

- 1) *A priori* region.
- 2) *A priori*-ambiguity transition region.
- 3) Ambiguity region.
- 4) Ambiguity-asymptotic transition region.
- 5) Asymptotic region.

The MSE achieved in the ambiguity region is determined by the envelope of the ACR. In Figs. 1(a) and 1(b), we denote by ρ_{pr} , ρ_{am1} , ρ_{am2} and ρ_{as} the *a priori*, begin-ambiguity, end-ambiguity and asymptotic thresholds delimiting the different regions. Note that the CRLB is achieved at high SNRs with asymptotically efficient estimators, such as the maximum likelihood estimator (MLE), only. Otherwise, the estimator achieves its own asymptotic MSE (e.g. MLE with random signals and finite snapshots [13, 14], Capon algorithm [15]).

The exact evaluation of the statistics, in the threshold region, of some estimators such as the MLE has been considered as a prohibitive task. Many lower bounds (LB) have been derived for both deterministic and Bayesian (when the unknown parameter follows a given *a priori* distribution)

parameters in order to be used as benchmarks and to describe the behavior of the MSE in the threshold region [16]. Some upper bounds (UB) have also been derived like the Seidman UB [17]. It will suffice to mention here [16, 18] the Cramer-Rao, Bhattacharyya, Chapman-Robbins, Barankin and Abel deterministic LBs, the Cramer-Rao, Bhattacharyya, Bobrovsky-MayerWolf-Zakai, Bobrovsky-Zakai, and Weiss-Weinstein Bayesian LBs, the Ziv-Zakai Bayesian LB (ZZLB) [2] with its improved versions: Bellini-Tartara [4], Chazan-Ziv-Zakai [19], Weinstein [20] (approximation of Bellini-Tartara), and Bell-Steinberg-Ephraim-VanTrees [21] (generalization of Ziv-Zakai and Bellini-Tartara), and the Reuven-Messer LB [22] for problems of simultaneously deterministic and Bayesian parameters.

The CRLB [23] gives the minimum MSE achievable by an unbiased estimator. However, it is very optimistic for low and moderate SNRs and does not indicate the presence of the threshold and ambiguity regions. The Barankin LB (BLB) [24] gives the greatest LB of an unbiased estimator. However, its general form is not easy to compute for most interesting problems. A useful form of this bound, which is much tighter than the CRLB, is derived in [25] and generalized to vector cases in [26]. The bound in [25] detects the asymptotic region much below the true one. Some applications of the BLB can be found in [3, 5, 8, 9, 27, 28].

The Bayesian ZZLB family [2, 4, 19–21] is based on the minimum probability of error of a binary detection problem. The ZZLBs are very tight; they detect the ambiguity region roughly and the asymptotic region accurately. Some applications of the ZZLBs, discussions and comparison to other bounds can be found in [10–12, 29–35].

In [36, pp. 627–637], Wozencraft considered time-of-arrival (TOA) estimation with cardinal sine waveforms and employed the method of interval estimation (MIE) to approximate the MSE of the MLE. The MIE [18, pp. 58–62] consists in splitting the *a priori* domain of the unknown parameter into intervals and computing the probability that the estimate falls in a given interval, and the estimator mean and variance in each interval. According to [18, 37], the MIE was first used in [38, 39] before Wozencraft [36] and others introduced some modifications later. The approach in [36] is imitated in [18, 37, 40, 41] for frequency estimation and in [42] for angle-of-arrival (AOA) estimation. The ACRs in [15, 18, 36, 37, 40–42] have the special shape of a cardinal sine (oscillating baseband with the mainlobe twice wider than the sidelobes); this limitation makes their approach inapplicable on other shapes. In [1], McAulay considered TOA estimation with carrier-modulated pulses (oscillating passband ACRs) and used the MIE to derive an approximate UB (AUB); the approach of McAulay can be applied to any oscillating ACR. Indeed, it is followed (independently apparently) in [15, 43, 44] for AOA estimation and in [41] (for frequency estimation as mentioned above) where it is compared to Wozencraft's approach. The ACR considered in [43, 44] has an arbitrary oscillating baseband shape (due to the use of non-regular arrays), meaning that it looks like a cardinal sine but with some strong sidelobes arbitrarily located. The MSEAs based on Wozencraft's approach are very accurate

and the AUBs using McAulay's approach are very tight in the asymptotic and threshold regions. Both approaches can be used to determine accurately the asymptotic region. Various estimators are considered in the aforementioned references. More technical details about the MIE are given in Sec. IV.

We consider the estimation of a scalar deterministic parameter. We employ the MIE to propose new approximations (rather than AUBs) of the MSE achieved by the MLE, which are highly accurate, and a very tight AUB. The MLE mean and probability density function (PDF) are approximated as well. More details about our contributions with regards to the MIE are given in Secs. IV and V. We derive an approximate LB (ALB) tighter than the CRLB based on the second order Taylor series expansion of noise. Also, we utilize the binary detection principle to derive some ALBs; the obtained bounds are very tight. The theoretical results presented in this paper are applicable to any estimation problem satisfying the system model introduced in Sec. II. In order to illustrate the accurateness of the proposed MSEAs and the tightness of the derived bounds, we consider the example of TOA estimation with baseband and passband pulses.

The materials presented in this paper compose the first part of our work divided in two parts [45, 46].

The rest of the paper is organized as follows. In Sec. II we introduce our system model. In Sec. III we describe the threshold and ambiguity phenomena. In Sec. IV we deal with the MIE. In Sec. V we propose an AUB and an MSEA. In Sec. VI we derive some ALBs. In Sec. VII we consider the example of TOA estimation and discuss the obtained numerical results.

II. SYSTEM MODEL

In this section we consider the general estimation problem of a deterministic scalar parameter (Sec. II-A) and the particular case of TOA estimation (Sec. II-B).

A. Deterministic scalar parameter estimation

Let Θ be a deterministic unknown parameter with $D_\Theta = [\Theta_1, \Theta_2]$ denoting its *a priori* domain. We can write the i th, ($i = 1, \dots, I$) observation as:

$$r_i(t) = \alpha s_i(t; \Theta) + \tilde{w}_i(t) \quad (1)$$

where $s_i(t; \Theta)$ is the i th useful signal carrying the information on Θ , α is a known positive gain, and $\tilde{w}_i(t)$ is an additive white Gaussian noise (AWGN) with two-sided power spectral density (PSD) of $\frac{N_0}{2}$; $\tilde{w}_1(t), \dots, \tilde{w}_I(t)$ are independent.

Denote by $E_x(\theta) = \sum_{i=1}^I \int_{-\infty}^{+\infty} x_i^2(t; \theta) dt$ the sum of the energies of $x_1(t; \theta), \dots, x_I(t; \theta)$, by \dot{x} and \ddot{x} the first and second derivatives of x w.r.t. θ , and by \mathbb{E} , \Re and \mathbb{P} the expectation, real part and probability operators respectively. From (1) we can write the log-likelihood function of Θ as:

$$\Lambda(\theta) = -\frac{1}{N_0} [E_r + \alpha^2 E_s(\theta) - 2\alpha X_{s,r}(\theta)] \quad (2)$$

where $\theta \in D_\Theta$ denotes a variable associated with Θ , and

$$X_{s,r}(\theta) = \sum_{i=1}^I \int_{-\infty}^{+\infty} s_i(t; \theta) r_i(t) dt = \alpha R_s(\theta, \Theta) + w(\theta) \quad (3)$$

is the crosscorrelation (CCR) with respect to (w.r.t.) θ , with

$$R_s(\theta, \theta') = \sum_{i=1}^I \int_{-\infty}^{+\infty} s_i(t; \theta) s_i(t; \theta') dt \quad (4)$$

denoting the ACR w.r.t. (θ, θ') and

$$w(\theta) = \sum_{i=1}^I \int_{-\infty}^{+\infty} s_i(t; \theta) \tilde{w}_i(t) dt \quad (5)$$

being a colored zero-mean Gaussian noise of covariance

$$C_w(\theta, \theta') = \sum_{i=1}^I \mathbb{E} \{w_i(\theta) w_i(\theta')\} = \frac{N_0}{2} R_s(\theta, \theta'). \quad (6)$$

1) *MLE, CRLB and envelope CRLB*: By assuming $E_s(\theta) = E_s$ in (2), that is, $E_s(\theta)$ is independent of θ , we can respectively write the MLE and the CRLB of Θ as [23, pp. 39]:

$$\hat{\Theta} = \underset{\theta \in D_\Theta}{\operatorname{argmax}} X_{s,r}(\theta) \quad (7)$$

$$c(\Theta) = \frac{-1}{\mathbb{E} \{ \ddot{\Lambda}(\theta) |_{\theta=\Theta} \}} = \frac{-N_0/2}{\alpha^2 \ddot{R}_s(\Theta, \Theta)} = \frac{1}{\rho \beta_s^2(\Theta)} \quad (8)$$

where

$$\rho = \frac{\alpha^2 E_s}{N_0/2} \quad (9)$$

$$\beta_s^2(\Theta) = -\frac{\ddot{R}_s(\Theta, \Theta)}{E_s} \quad (10)$$

denote the SNR and the normalized curvature of $R_s(\theta, \Theta)$ at $\theta = \Theta$ respectively. Unlike $E_s(\Theta)$, $\ddot{R}_s(\Theta, \Theta)$ may depend on Θ (e.g., AOA estimation [47]). The CRLB in (8) is inversely proportional to the curvature of the ACR at $\theta = \Theta$. Sometimes $R_s(\theta, \Theta)$ is oscillating w.r.t. θ . Then, if the SNR is sufficiently high (resp. relatively low) the maximum of the CCR in (3) will fall around the global maximum (resp. the local maxima) of $R_s(\theta, \Theta)$ and the MLE in (7) will (resp. will not) achieve the CRLB. We will see in Sec. VII that the MSE achieved at medium SNRs is inversely proportional to the curvature of the envelope of the ACR instead of the curvature of the ACR itself. To characterize this phenomenon known as “ambiguity” [48] we will define below the envelope CRLB (ECRLB).

Denote by f the frequency² relative to θ and define the Fourier transform (FT), the mean frequency and the complex envelope w.r.t. $f_c(\Theta)$ of $R_s(\theta, \Theta)$ respectively by

$$\mathcal{F}_{R_s}(f) = \int_{\Theta_1}^{\Theta_2} R_s(\theta, \Theta) e^{-j2\pi f(\theta-\Theta)} d\theta \quad (11)$$

$$f_c(\Theta) = \frac{\int_0^{+\infty} f \Re \{ \mathcal{F}_{R_s}(f) \} df}{\int_0^{+\infty} \Re \{ \mathcal{F}_{R_s}(f) \} df} \quad (12)$$

$$R_s(\theta, \Theta) = \Re \left\{ e^{j2\pi(\theta-\Theta)f_c(\Theta)} e_{R_s}(\theta, \Theta) \right\}. \quad (13)$$

In Appendix A we show that:

$$-\ddot{R}_s(\Theta, \Theta) = -\Re \{ \ddot{e}_{R_s}(\Theta, \Theta) \} + 4\pi^2 f_c^2(\Theta) E_s. \quad (14)$$

Now, we define the ECRLB as:

$$c_e(\Theta) = -\frac{N_0/2}{\alpha^2 \Re \{ \ddot{e}_{R_s}(\Theta, \Theta) \}} = \frac{1}{\rho \beta_e^2(\Theta)} \quad (15)$$

²E.g., f is in seconds (resp. Hz) for frequency (resp. TOA) estimation.

where

$$\beta_e^2(\Theta) = -\frac{\Re \{ \ddot{e}_{R_s}(\Theta, \Theta) \}}{E_s} \quad (16)$$

denotes the normalized curvature of $e_{R_s}(\theta, \Theta)$ at $\theta = \Theta$. From (10), (14) and (16), we have:

$$\beta_s^2(\Theta) = \beta_e^2(\Theta) + 4\pi^2 f_c^2(\Theta). \quad (17)$$

2) *BLB*: The BLB can be written as [25]:

$$c_B = (\underline{\Theta} - \Theta)^T D^{-1} (\underline{\Theta} - \Theta) \quad (18)$$

where

$$\begin{aligned} \underline{\Theta} &= (\theta_{n_1} \cdots \theta_{-1} \ 1 + \Theta \ \theta_1 \cdots \theta_{n_N})^T \\ D &= (d_{i,j})|_{i,j=n_1, \dots, n_N} \end{aligned}$$

with $\theta_{n_1}, \dots, \theta_{n_N}$ ($n_1 \leq 0, n_N \geq 0, \theta_0 = \Theta$) denoting N testpoints in the *a priori* domain of Θ , and³

$$d_{0,0} = \frac{\alpha^2 E_s(\Theta)}{N_0/2} = \frac{1}{c(\Theta)}$$

$$d_{0,i \neq 0} = d_{i,0} = \frac{\alpha^2}{N_0/2} [\dot{R}_s(\Theta, \theta_i) - \dot{R}_s(\Theta, \Theta)]$$

$$d_{i \neq 0, j \neq 0} = \frac{\alpha^2}{N_0/2} [R_s(\theta_i, \theta_j) - R_s(\theta_i, \Theta) - R_s(\theta_j, \Theta) + E_s].$$

3) *Maximum MSE*: The maximum MSE

$$e_U = \sigma_U^2 + (\Theta - \mu_U)^2 \quad (19)$$

with $\mu_U = \frac{\Theta_1 + \Theta_2}{2}$ and $\sigma_U^2 = \frac{(\Theta_2 - \Theta_1)^2}{12}$ is achieved when the estimator becomes uniformly distributed in D_Θ [30, 34].

The system model considered in this subsection is satisfied for various estimation problems such as TOA, AOA, phase, frequency and velocity estimation. Therefore, the theoretical results presented in this paper are valid for the different mentioned parameters. TOA is just considered as an example to validate the accurateness and the tightness of our MSEAs and upper and lowers bounds.

B. Example: TOA estimation

With TOA estimation based on one observation ($I = 1$), $s_1(t; \Theta)$ in (1) becomes $s_1(t; \Theta) = s(t - \Theta)$ where $s(t)$ denotes the transmitted signal and Θ represents the delay introduced by the channel. Accordingly, we can write the ACR in (4) as $R_s(\theta, \theta') = R_s(\theta - \theta')$ where $R_s(\theta) = \int_{-\infty}^{+\infty} s(t + \theta) s(t) dt$, and the CCR in (3) as:

$$X_{s,r}(\theta) = \alpha R_s(\theta - \Theta) + w(\theta). \quad (20)$$

The CRLB $c(\Theta)$ in (8), ECRLB $c_e(\Theta)$ in (15), mean frequency $f_c(\Theta)$ in (12), normalized curvatures $\beta_s^2(\Theta)$ in (10) and $\beta_e^2(\Theta)$ in (16) become now all independent of Θ . Furthermore, β_s^2 and β_e^2 denote now the mean quadratic bandwidth (MQBW) and the envelope MQBW (EMQBW) of $s(t)$ respectively.

The CRLB in (8) is much smaller than the ECRLB in (15) because the MQBW in (17) is much larger than the EMQBW in (16). In fact, for a signal occupying the whole band from 3.1 to 10.6 GHz⁴ ($f_c = 6.85$ GHz, bandwidth $B = 7.5$

³We can show that $E_s(\theta) = -\ddot{R}_s(\theta, \Theta)$ if $E_s(\theta)$ is independent from θ .

⁴The ultra wideband (UWB) spectrum authorized for unlicensed use by the US federal commission of communications in May 2002 [49].

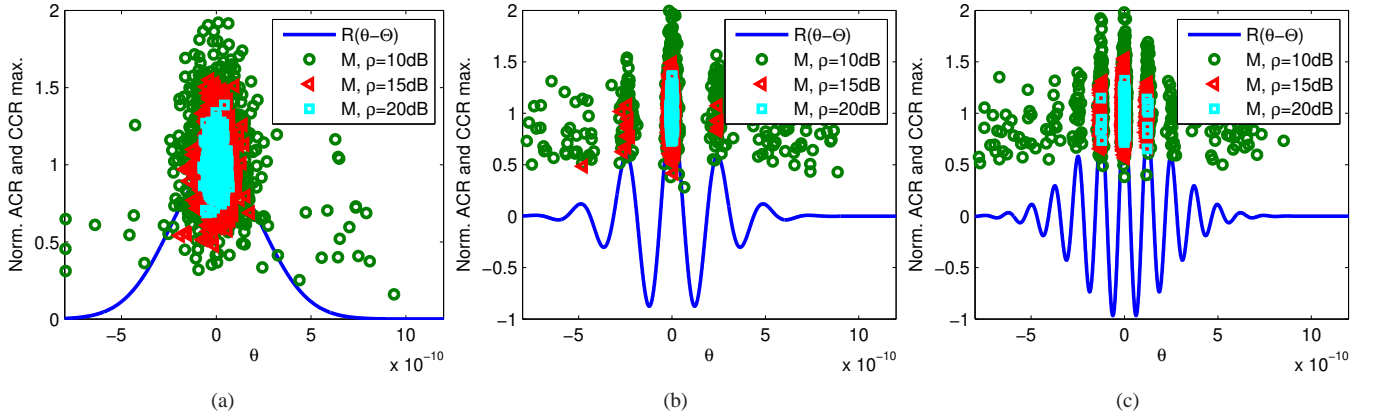


Figure 2. Normalized ACR $R(\theta - \Theta)$ and 1000 realizations of $M[\hat{\Theta}, X(\hat{\Theta})]$ per SNR ($\rho = 10, 15$ and 20 dB); Gaussian pulse modulated by f_c , $\Theta = 0$ ns, $T_w = 0.6$ ns, $D_\Theta = [-1.5, 1.5]T_w$ (a) $f_c = 0$ GHz (b) $f_c = 4$ GHz (c) $f_c = 8$ GHz.

GHz), we obtain $\beta_e^2 = \frac{\pi^2 B^2}{3} \approx 185 \text{ GHz}^2$, $4\pi^2 f_c^2 \approx 10\beta_e^2$, $\beta_s^2 \approx 11\beta_e^2$ and $c \approx \frac{c_e}{11}$. Therefore, the estimation performance seriously deteriorates at relatively low SNRs when the ECRLB is achieved instead of the CRLB due to ambiguity.

III. THRESHOLD AND AMBIGUITY PHENOMENA

In this section we explain the physical origin of the threshold and ambiguity phenomena by considering TOA estimation with UWB pulses⁵ as an example. The transmitted signal

$$s(t) = 2sqr t \frac{E_s}{T_w} e^{-2\pi \frac{t^2}{T_w}} \cos(2\pi f_c t) \quad (21)$$

is a Gaussian pulse of width T_w modulated by a carrier f_c . We consider three values of f_c ($f_c = 0, 4$ and 8 GHz) and three values of the SNR ($\rho = 10, 15$ and 20 dB) per considered f_c . We take $\Theta = 0$, $T_w = 0.6$ ns, and $D_\Theta = [-1.5, 1.5]T_w$.

In Figs. 2(a)–2(c) we show the normalized ACR $R(\theta - \Theta) = \frac{R_s(\theta - \Theta)}{E_s}$ for $f_c = 0$ (baseband pulse), 4 and 8 GHz (passband pulses) respectively, and 1000 realizations per SNR of the maximum $M[\hat{\Theta}, X(\hat{\Theta})]$ of the normalized CCR $X(\theta) = \frac{X_{s,r}(\theta)}{\alpha E_s}$. Denote by N_n , ($n = n_1, \dots, n_N$), (N is the number of local maxima in D_Θ), ($n_1 < 0$, $n_N > 0$), ($n = 0$ corresponds to the global maximum) the number of samples of M falling around the n th local maximum (i.e. between the two local minima adjacent to that maximum) of $R(\theta - \Theta)$. In Table I, we show w.r.t. f_c and ρ the number of samples falling around the maxima number 0 and 1 , the CRLB square root (SQRT) \sqrt{c} of Θ , the root MSE (RMSE) $\sqrt{e_S}$ obtained by simulation and the RMSE to CRLB SQRT ratio $\sqrt{\frac{e_S}{c}}$.

Consider first the baseband pulse. We can see in Fig. 2(a) that the samples of M are very close to the maximum of $R(\theta - \Theta)$ for $\rho = 20$ dB, and they start to spread progressively along $R(\theta - \Theta)$ for $\rho = 15$ and 10 dB. Table I shows that the CRLB is approximately achieved for $\rho = 20$ and 15 dB, but not for $\rho = 10$ dB. Based on this observation, we can describe the threshold phenomenon as follows. For sufficiently

f_c	ρ	\sqrt{c}	$\sqrt{e_S}$	$\sqrt{\frac{e_S}{c}}$	N_0	N_1
0	10	76	123	1.61	1000	0
	15	43	46	1.10	1000	0
	20	24	24	1.01	1000	0
4	10	12	196	15.81	773	59
	15	7	31	4.47	985	8
	20	4	4	1.01	1000	0
8	10	6.3	198	31.56	481	199
	15	3.5	50	14.35	838	75
	20	2	14	7.14	987	7

Table I
CRLB SQRT \sqrt{c} (PS), SIMULATED RMSE $\sqrt{e_S}$ (PS), RMSE TO CRLB SQRT RATIO $\sqrt{\frac{e_S}{c}}$, AND NUMBER (N_0, N_1) OF THE M SAMPLES FALLING AROUND THE MAXIMA NUMBER 0 AND 1 , FOR $f_c = 0, 4$ AND 8 GHz, AND $\rho = 10, 15$ AND 20 dB.

high SNRs (resp. relatively low SNRs), the maximum of the CCR falls in the vicinity of the maximum of the ACR (resp. spreads along the ACR) so the CRLB is (resp. is not) achieved.

Consider now the pulse with $f_c = 4$ GHz. Fig. 2(b) and Table I show that for $\rho = 20$ dB all the samples of M fall around the global maximum of $R(\theta - \Theta)$ and the CRLB is achieved, whereas for $\rho = 15$ and 10 dB they spread along the local maxima of $R(\theta - \Theta)$ and the achieved MSE is much larger than the CRLB. Based on this observation, we can describe the ambiguity phenomenon as follows. For sufficiently high SNRs (resp. relatively low SNRs) the noise component $w(t)$ in the CCR $X_{s,r}(\theta)$ in (20) is not (resp. is) sufficiently high to fill the gap between the global maximum and the local maxima of the ACR. Consequently, for sufficiently high SNRs (resp. relatively low SNRs) the maximum of the CCR always falls around the global maximum (resp. spreads along the local maxima) of the ACR so the CRLB is (resp. is not) achieved. Obviously, the ambiguity phenomenon affects the threshold phenomenon because the SNR required to achieve the CRLB depends on the gap between the global and the local maxima.

Let us now examine the RMSE achieved at $\rho = 20$ dB for $f_c = 4$ and 8 GHz; it is 3.5 times smaller with $f_c = 4$ GHz than with $f_c = 8$ GHz whereas the CRLB SQRT is 2 times smaller with the latter. In fact, the samples of M do

⁵ We chose UWB pulses because they can achieve the CRLB at relatively low SNRs thanks to their relatively high fractional bandwidth (bandwidth to central frequency ratio).

not fall all around the global maximum for $f_c = 8$ GHz. This amazing result (observed in [50] from experimental results) exhibits the significant loss in terms of accuracy if the CRLB is not achieved due to ambiguity. It also shows the necessity to design our system such that the CRLB be attained.

IV. MIE-BASED MLE STATISTICS APPROXIMATION

We have seen in Sec. III that the threshold phenomenon is due to the spreading of the estimates along the ACR. To characterize this phenomenon we split the *a priori* domain D_Θ into N intervals $D_n = [d_n, d_{n+1})$, ($n = n_1, \dots, n_N$), ($n_1 \leq 0, n_N \geq 0$) and write the PDF, mean and MSE of $\hat{\Theta}$ as

$$\begin{aligned} p(\theta) &= \sum_{n=n_1}^{n_N} P_n p_n(\theta) \\ \mu &= \int_{\Theta_1}^{\Theta_2} \theta p(\theta) d\theta = \sum_{n=n_1}^{n_N} P_n \mu_n \\ e &= \int_{\Theta_1}^{\Theta_2} (\theta - \Theta)^2 p(\theta) d\theta = \sum_{n=n_1}^{n_N} P_n [(\Theta - \mu_n)^2 + \sigma_n^2] \end{aligned} \quad (22)$$

where

$$\begin{aligned} P_n &= \mathbb{P}\{\hat{\Theta} \in D_n\} \\ &= \mathbb{P}\{\exists \xi \in D_n : X_{s,r}(\xi) > X_{s,r}(\theta), \forall \theta \in \cup_{n' \neq n} D_{n'}\} \end{aligned} \quad (23)$$

denotes the interval probability (i.e. probability that $\hat{\Theta}$ falls in D_n), and $p_n(\theta)$, $\mu_n = \mathbb{E}\{\hat{\Theta}_n\}$ and $\sigma_n^2 = \mathbb{E}\{(\hat{\Theta}_n - \mu_n)^2\}$ represent, respectively, the PDF, mean and variance of the interval MLE ($\hat{\Theta}$ given $\hat{\Theta} \in D_n$)

$$\hat{\Theta}_n = \hat{\Theta} | \hat{\Theta} \in D_n. \quad (24)$$

Denote by θ_n a testpoint selected in D_n and let $X_n = X_{s,r}(\theta_n) = \alpha R_n + w_n$ with $R_n = R_s(\theta_n, \Theta)$ and $w_n = w(\theta_n)$. Using (3), P_n in (23) can be approximated by

$$\begin{aligned} \tilde{P}_n &= \mathbb{P}\{X_n > X_{n'}, \forall n' \neq n\} = \int_{-\infty}^{+\infty} dx_n \int_{-\infty}^{x_n} dx_{n_1} \dots \\ &\quad \int_{-\infty}^{x_n} dx_{n-1} \int_{-\infty}^{x_n} dx_{n+1} \dots \int_{-\infty}^{x_n} p_X(x) dx_{n_N} \end{aligned} \quad (25)$$

where

$$p_X(x) = \frac{1}{(2\pi)^{\frac{N}{2}} |C_X|^{\frac{1}{2}}} e^{-\frac{(x - \mu_X) C_X^{-1} (x - \mu_X)^T}{2}}$$

represents the PDF of $X = (X_{n_1} \dots X_{n_N})^T$ with $\mu_X = (\mu_{X_{n_1}} \dots \mu_{X_{n_N}})^T = \alpha(R_{n_1} \dots R_{n_N})^T$ being its mean and $C_X = \frac{N_0}{2} [R_s(\theta_n, \theta_{n'})]_{n,n'=n_1, \dots, n_N}$ its covariance matrix.

The accuracy of the approximation in (25) depends on the choice of the intervals and the testpoints. For an oscillating ACR we consider an interval around each local maximum and choose the abscissa of the local maximum as a testpoint, whereas for a non-oscillating ACR we split D_Θ into equal intervals and choose the center $\theta_n = \frac{d_n + d_{n+1}}{2}$ of each interval as a testpoint. For both oscillating and non-oscillating ACRs, D_0 contains the global maximum and θ_0 is equal to Θ .

The testpoints are chosen as the roots of the ACR (except for $\theta_0 = \Theta$) in [18, 36, 37, 40–42], as the local extrema abscissa in [1], and as the local maxima abscissa in [15, 41, 43, 44].

A. Computation of the interval probability

We consider here the computation of the approximate interval probability \tilde{P}_n in (25).

1) *Numerical approximation:* To the best of our knowledge there is no closed form expression for the integral in (25) for correlated X_n . However, it can be computed numerically using for example the MATLAB function QSCMVNV (written by Genz based on [51–54]) that computes the multivariate normal probability with integration region specified by a set of linear inequalities in the form $b_1 < B(X - \mu_X) < b_2$. Using QSCMVNV, \tilde{P}_n can be approximated by:

$$P_n^{(1)} = \text{QSCMVNV}(N_p, C_X, b_1, B, b_2) \quad (26)$$

where N_p is the number of points used by the algorithm (e.g. $N_p = 3000$), $b_1 = (-\infty \dots -\infty)^T$ and $b_2 = \mu_{X_n} - (\mu_{X_{n_1}} \dots \mu_{X_{n-1}} \mu_{X_{n+1}} \dots \mu_{X_{n_N}})^T$ two $(N-1)$ -column vectors, and $B = \begin{pmatrix} B_1 & B_2 & B_3 & B_4 & B_5 \end{pmatrix}$ an $(N-1) \times N$ matrix with $B_1 = I(n - n_1)$, $B_2 = \text{zeros}(N + n_1 - n - 1, n - n_1)$, $B_3 = -\text{ones}(N - 1, 1)$, $B_4 = \text{zeros}(N - n_N + n - 1, n_N - n)$ and $B_5 = I(n_N - n)^6$.

2) *Analytic approximation:* Denote by $Q(y) = \frac{1}{\sqrt{2\pi}} \int_y^\infty e^{-\frac{\xi^2}{2}} d\xi$ the Q function. As $\mathbb{P}\{A_1 \cap A_2\} \leq \mathbb{P}\{A_1\}$, we can upper bound \tilde{P}_n in (25) by:

$$P_n^{(2)} = \begin{cases} P(\theta_0, \theta_1) & n = 0 \\ P(\theta_n, \theta_0) & n \neq 0 \end{cases} \quad (27)$$

where

$$\begin{aligned} P(\theta, \theta') &= \mathbb{P}\{X_{s,r}(\theta) > X_{s,r}(\theta')\} \\ &= Q\left(\sqrt{\frac{\rho}{2}} \frac{R(\theta', \Theta) - R(\theta, \Theta)}{\sqrt{1 - R(\theta, \theta')}}\right) \end{aligned} \quad (28)$$

with $R(\theta, \Theta) = \frac{R_s(\theta, \Theta)}{B_s}$ denoting the normalized ACR. $P(\theta, \theta')$ is obtained (28) from (3) and (6) by noticing that $X_{s,r}(\theta) - X_{s,r}(\theta') \sim \mathcal{N}(\alpha[R_s(\theta, \Theta) - R_s(\theta', \Theta)], N_0[E_s - R_s(\theta, \theta')])^7$. If N approaches infinity, then both $\sum_{n=n_1}^{n_N} P_n^{(2)}$ and the MSEA in (22) will approach infinity.

Using (27), we propose the following approximation:

$$P_n^{(3)} = \frac{P_n^{(2)}}{\sum_{n=n_1}^{n_N} P_n^{(2)}}. \quad (29)$$

In this subsection we have seen that the interval probability P_n in (23) can be approximated by $P_n^{(1)}$ in (26) or $P_n^{(3)}$ in (29), and upper bounded by $P_n^{(2)}$ in (27).

The UB $P_n^{(2)}$ is adopted in [1, 15, 41, 43, 44] with minor modifications; in fact, \tilde{P}_0 is approximated by one in [1] and by $1 - \sum_{n \neq 0} P_n^{(2)}$ in [15, 41, 43, 44]. In the special case where $X_{n_1}, \dots, X_{-1}, X_1, \dots, X_{n_N}$ are independent and identically distributed such as in [18, 36, 37, 40–42] thanks to the cardinal sine ACR, then $\tilde{P}_n = \frac{\tilde{P}_A}{N-1}$, $\forall n \neq 0$, and $\tilde{P}_0 = 1 - \tilde{P}_A$ (\tilde{P}_A is the approximate probability of ambiguity); consequently,

⁶We denote by $I(k)$ the identity matrix of rank k , and $\text{zeros}(k_1, k_2)$ and $\text{ones}(k_1, k_2)$ the zero and one matrices of dimension $k_1 \times k_2$.

⁷ $\mathcal{N}(m, v)$ stands for the normal distribution of mean m and variance v .

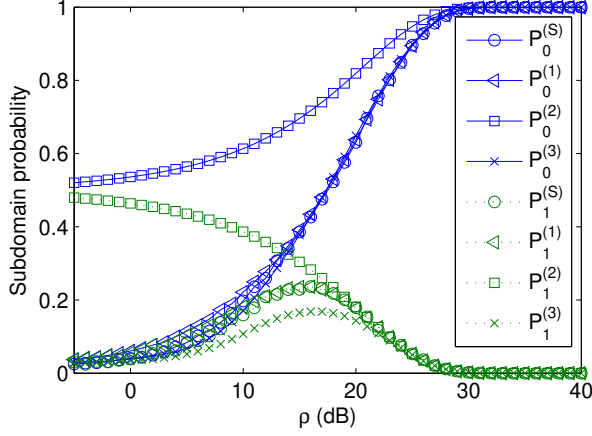


Figure 3. Simulated interval probability $P_n^{(S)}$, the approximations $P_n^{(1)}$ and $P_n^{(3)}$, and the AUB $P_n^{(2)}$ for $n = 0, 1$ w.r.t. the SNR.

the MSEA in (22) can be written as the sum of two terms: $e \approx \tilde{P}_{AEU} + \tilde{P}_0 c(\Theta)$; \tilde{P}_0 can be calculated by performing one-dimensional integration. If $X_0 \sim \mathcal{N}(\alpha E_s, \frac{N_0}{2} E_s)$ and $X_n \sim \mathcal{N}(0, \frac{N_0}{2} E_s)$, $\forall n \neq 0$, like in [18, 36, 37, 41] then P_A can be upper bounded using the union bound [36].

As an example, to evaluate the accurateness of $P_n^{(1)}$ in (26) and $P_n^{(3)}$ in (29) and to compare them to $P_n^{(2)}$ in (27), we consider the pulse in (21) with $f_c = 6.85$ GHz, $T_w = 2$ ns, $\Theta = 0$ and $D_\Theta = [-2, 1.5]T_w$. In Fig. 3 we show for $n = 0$ and 1, the interval probability $P_n^{(S)}$ obtained by simulation based on 10000 trials, $P_n^{(1)}$, $P_n^{(2)}$ and $P_n^{(3)}$, all versus the SNR. We can see that $P_n^{(S)}$ converges to $\frac{1}{N}$ at low SNRs for all intervals; however, it converges to 1 at high SNRs ($P_0^S = 0.99$ for $\rho \approx 30$ dB) for $n = 0$ (probability of non-ambiguity) and to 0 for $n \neq 0$. Both $P_n^{(1)}$ and $P_n^{(3)}$ are very accurate and closely follow $P_n^{(S)}$. The UB $P_n^{(2)}$ is not tight at low SNRs; it converges to 0.5 $\forall n$ instead of $\frac{1}{N}$ due to (28). However, it converges to 1 (resp. 0) for $n = 0$ (resp. $n \neq 0$) at high SNRs simultaneously with $P_n^{(S)}$ so it can be used to determine accurately the asymptotic region.

B. Statistics of the interval MLE

We approximate here the statistics of the interval MLE $\hat{\Theta}_n$ in (24). We have already mentioned in Sec. IV that for an oscillating (resp. a non-oscillating) ACR we consider an interval around each local maximum (resp. split the *a priori* domain into equal intervals); the global maximum is always contained in D_0 . Accordingly, the ACR inside a given interval is either increasing then decreasing or monotone (i.e. increasing, decreasing or constant).

As the distribution of $\hat{\Theta}_n$ should follow the shape of the ACR in the considered interval, the interval variance is upper bounded by the variance of uniform distribution in $D_n = [d_n, d_{n+1}]$. Therefore, the interval mean μ_n and variance σ_n^2 can be approximated by

$$\mu_{n,U} = \frac{d_n + d_{n+1}}{2} \quad (30)$$

$$\sigma_{n,U}^2 = \frac{(d_{n+1} - d_n)^2}{12}. \quad (31)$$

For intervals with local minima (not considered here), the ACR decreases then increases so σ_n^2 is upper bounded by the variance of a Bernoulli distribution of two equiprobable atoms:

$$\sigma_{n,\max}^2 = \frac{(d_{n+1} - d_n)^2}{4} > \sigma_{n,U}^2. \quad (32)$$

In [1], it is assumed that σ_n^2 is upper bounded by $\sigma_{i,U}^2$ in (31) even for intervals with local minima. See [55, 56] for further information on the maximum variance.

The CCR $X_{s,r}(\theta)$ in (3) can be approximated inside D_n by its Taylor series expansion about θ_n limited to second order:

$$\begin{aligned} X_{s,r}(\theta) &= \alpha R_s(\theta, \Theta) + w(\theta) \\ &\approx (\alpha \dot{R}_n + w_n) + (\alpha \ddot{R}_n + \ddot{w}_n)(\theta - \theta_n) \\ &\quad + (\alpha \ddot{R}_n + \ddot{w}_n) \frac{(\theta - \theta_n)^2}{2} \end{aligned} \quad (33)$$

where $\dot{w}_n = \dot{w}(\theta_n)$, $\ddot{w}_n = \ddot{w}(\theta_n)$, $\dot{R}_n = \dot{R}_s(\theta_n, \Theta)$ and $\ddot{R}_n = \ddot{R}_s(\theta_n, \Theta)$. Let ν_n be the correlation coefficient of \dot{w}_n and \ddot{w}_n . Then, from (5), we can show that

$$\dot{w}_n \sim \mathcal{N}(0, \sigma_{\dot{w}_n}^2) \quad (34)$$

$$\ddot{w}_n \sim \mathcal{N}(0, \sigma_{\ddot{w}_n}^2) \quad (35)$$

with

$$\sigma_{\dot{w}_n}^2 = \frac{N_0}{2} \int_{-\infty}^{+\infty} \dot{s}^2(t; \theta_n) dt = \frac{N_0}{2} E_{\dot{s}}(\theta_n) \quad (36)$$

$$\sigma_{\ddot{w}_n}^2 = \frac{N_0}{2} \int_{-\infty}^{+\infty} \ddot{s}^2(t; \theta_n) dt = \frac{N_0}{2} E_{\ddot{s}}(\theta_n) \quad (37)$$

$$\nu_n = \frac{\mathbb{E}\{\dot{w}_n \ddot{w}_n\}}{\sigma_{\dot{w}_n} \sigma_{\ddot{w}_n}} = \frac{\int_{-\infty}^{+\infty} \dot{s}(t; \theta_n) \ddot{s}(t; \theta_n) dt}{\sqrt{E_{\dot{s}}(\theta_n) E_{\ddot{s}}(\theta_n)}}. \quad (38)$$

Let us first consider an interval with monotone ACR. By neglecting \ddot{w}_n and \ddot{R}_n in (33) (linear approximation), we can approximate the interval MLE by:

$$\begin{aligned} \hat{\Theta}_n &= \operatorname{argmax}_{\theta \in D_n} \{X_{s,r}(\theta)\} \\ &\approx \begin{cases} d_n & \alpha \dot{R}_n + \dot{w}_n < 0 \\ d_{n+1} & \alpha \dot{R}_n + \dot{w}_n > 0 \\ \frac{d_{n,1} + d_{n,2}}{2} & \alpha \dot{R}_n + \dot{w}_n = 0. \end{cases} \end{aligned} \quad (39)$$

As $\mathbb{P}\{\alpha \dot{R}_n + \dot{w}_n = 0\} = 0$, the latter approximation follows a two atoms Bernoulli distribution with probability, mean and variance given from (9), (34) and (36) by:

$$\begin{aligned} \mathbb{P}\{d_n\} &= 1 - \mathbb{P}\{d_{n+1}\} = \mathbb{P}\{-\dot{w}_n > \alpha \dot{R}_n\} \\ &= Q\left(\frac{\alpha \dot{R}_n}{\sigma_{\dot{w}_n}}\right) = Q\left(\sqrt{\frac{\rho \dot{R}_n^2}{E_s E_{\dot{s}}(\theta_n)}}\right) \\ \mu_{n,B} &= d_n \mathbb{P}\{d_n\} + d_{n+1} \mathbb{P}\{d_{n+1}\} \\ \sigma_{n,B}^2 &= \mathbb{P}\{d_n\} \mathbb{P}\{d_{n+1}\} (d_{n+1} - d_n)^2 \end{aligned} \quad (40)$$

where $\sigma_{n,B}^2$ is upper bounded by $\sigma_{n,\max}^2$ in (32) and reaches it for $\mathbb{P}\{d_n\} = 0.5$; $\mathbb{P}\{d_n\} = 0.5$ just means that $\hat{\Theta}_n$ is uniformly distributed in D_n (because $\hat{\Theta}_n$ can fall anywhere inside D_n); therefore, μ_n and σ_n^2 can be approximated by:

$$\mu_{n,1,c} = \mu_{n,B} \quad (41)$$

$$\sigma_{n,1,c}^2 = \min\{\sigma_{n,U}^2, \sigma_{n,B}^2\}. \quad (42)$$

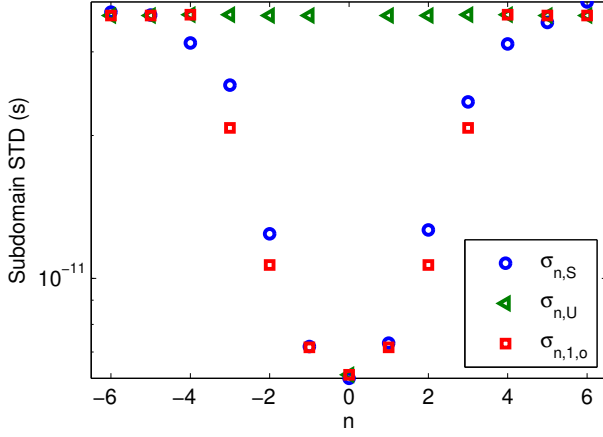


Figure 4. Simulated interval STD $\sigma_{n,S}$ and approximations $\sigma_{n,U}$ and $\sigma_{n,1,o}$ w.r.t. the interval number $n = -6, \dots, 6$ for $\rho = 10$ dB.

By neglecting \dot{w}_n in (33) and (39) (because $\sigma_n^2 \ll (\Theta - \mu_n)^2$ for $n \neq 0$, see (22)) we obtain the following approximation:

$$\mu_{n,2,c} = \begin{cases} d_n & \dot{R}_n < 0 \\ d_{n+1} & \dot{R}_n > 0 \\ \frac{d_n + d_{n+1}}{2} & \dot{R}_n = 0 \end{cases} \quad (43)$$

$$\sigma_{n,2,c}^2 = 0. \quad (44)$$

Consider now an interval with a local maximum. By neglecting \dot{w}_n in (33), and taking into account that $\dot{R}_n = 0$ (local maximum), $\hat{\Theta}_n$ can be approximated by:

$$\hat{\Theta}_n = \operatorname{argmax}_{\theta \in D_n} \{X_{s,r}(\theta)\} \approx \theta_n - \frac{\dot{w}_n}{\alpha \ddot{R}_n} \quad (45)$$

which follows a normal distribution whose PDF, mean and variance can be obtained from (8), (34), (36) and (45):

$$p_{n,N}(\theta) = \frac{1}{\sqrt{2\pi}\sigma_{n,N}} e^{-\frac{(\theta - \mu_{n,N})^2}{2\sigma_{n,N}^2}} \quad (46)$$

$$\mu_{n,N} = \theta_n \quad (47)$$

$$\sigma_{n,N}^2 = \frac{\sigma_{\dot{w}_n}^2}{\alpha^2 \ddot{R}_n^2} = \frac{\frac{N_0}{2} E_s(\theta_n)}{\alpha^2 \ddot{R}_n^2} = c \frac{-\ddot{R}_0 E_s(\theta_n)}{\ddot{R}_n^2}. \quad (48)$$

For $n = 0$, $\sigma_{n,N}^2$ is equal to the CRLB in (8) since $-\ddot{R}_0 = E_s(\theta_0)$. To take into account that D_n is finite, we propose from (46), (47) and (48) the following approximation:

$$\mu_{n,1,o} = \int_{d_n}^{d_{n+1}} \theta p_{n,1,o}(\theta) d\theta \approx \theta_n \quad (49)$$

$$\begin{aligned} \sigma_{n,1,o}^2 &= \int_{d_n}^{d_{n+1}} (\theta - \mu_{n,1,o})^2 p_{n,1,o}(\theta) d\theta \\ &\approx \min\{\sigma_{n,N}^2, \sigma_{n,U}^2\} \end{aligned} \quad (50)$$

where $p_{n,1,o}(\theta) = \frac{p_{n,N}(\theta)}{\int_{d_n}^{d_{n+1}} p_{n,N}(\theta) d\theta}$. By neglecting $w(\theta)$ in (33) and (45), we obtain the following approximation:

$$\mu_{n,2,o} = \theta_n \quad (51)$$

$$\sigma_{n,2,o}^2 = 0. \quad (52)$$

For both oscillating and non-oscillating ACRs, D_0 contains the global maximum. To guarantee the convergence of the

MSEA in (22) to the CRLB, μ_0 and σ_0^2 should always be approximated using (49) and (50) by:

$$\mu_{0,0} = \Theta \quad (53)$$

$$\sigma_{0,0}^2 = \min\{c, \sigma_{0,U}^2\}. \quad (54)$$

For TOA estimation, we can write (40) and (48) as $\mathbb{P}\{d_n\} = Q\left(\sqrt{\rho} \frac{\dot{R}_n}{E_s \beta_s}\right)$ and $\sigma_{n,N}^2 = c \frac{\ddot{R}_n^2}{R_n^2}$.

We have seen in this subsection that the interval mean and variance can be approximated by

- $\mu_{0,0}$ in (53) and $\sigma_{0,0}^2$ in (54) for $n = 0$.
- $\mu_{n,U}$ in (30) and $\sigma_{n,U}^2$ in (31), $\mu_{n,1,c}$ in (41) and $\sigma_{n,1,c}^2$ in (42), or $\mu_{n,2,c}$ in (43) and $\sigma_{n,2,c}^2$ in (44) for intervals with monotone ACR.
- $\mu_{n,U}$ and $\sigma_{n,U}^2$, $\mu_{n,1,o}$ in (49) and $\sigma_{n,1,o}^2$ in (50), or $\mu_{n,2,o}$ in (51) and $\sigma_{n,2,o}^2$ in (52) for intervals with local maxima.

In [18, 36, 37, 40, 42] (resp. [15, 41, 43, 44]) σ_n^2 is approximated by $\sigma_{n,U}^2$ (resp. $\sigma_{n,2,o}^2$). They all approximate μ_n by θ_n and σ_0^2 by the asymptotic MSE (equal to the CRLB if the considered estimator is asymptotically efficient).

To evaluate the accurateness of $\sigma_{n,U}^2$ in (31) and $\sigma_{n,1,o}^2$ in (50), we consider the pulse in (21) with $f_c = 8$ GHz, $T_w = 0.6$ ns, $D_\Theta = [-1.5, 1.5]T_w$ and $\rho = 10$ dB. In Fig. 4 we show the approximate interval standard deviations (STD) $\sigma_{n,U}$ and $\sigma_{n,1,o}$, and the STD $\sigma_{n,S}$ obtained by simulation based on 50000 trials, w.r.t. the interval number $n = -6, \dots, 6$. We can see that $\sigma_{n,S}$ is upper bounded by $\sigma_{n,U}$ as expected and that $\sigma_{n,1,o}$ follows $\sigma_{n,S}$ closely. The smallest variance corresponds to $n = 0$ because the curvature of $R_s(\theta, \Theta)$ reaches its maximum at $\theta = \Theta$.

Before ending this section, we would like to highlight our contributions regarding the MIE. We have proposed two approximations for the interval probability when X_{n_1}, \dots, X_{n_N} are correlated. We have shown in Fig. 3 how our approximations are accurate. To the best of our knowledge all previous authors adopt the McAulay probability UB (except for the case where X_{n_1}, \dots, X_{n_N} are independent thanks to the cardinal sine ACR). We have proposed two new approximations for the interval mean and variance, one for intervals with monotone ACRs and one for intervals with local maxima. We have seen in Fig. 4 how our approximations are accurate. To the best of our knowledge all previous authors either upper bound the interval variance or neglect it. Thanks to the proposed probability approximations our MSEAs (e.g. $e_{1,1,c}$ in Fig. 6) are highly accurate and outperform the MSE UB of McAulay ($e_{2,U}$ in Fig. 7) and thanks to the proposed interval variance approximations the MSEA is improved ($e_{1,U}$ and $e_{1,2,c}$ outperform $e_{1,1,c}$ in Fig. 6). We have applied the MIE to non-oscillating ACRs. To the best of our knowledge this case is not considered before.

V. AN AUB AND AN MSEA BASED ON THE INTERVAL PROBABILITY

In this section we propose an AUB (Sec. V-A) and an MSEA (Sec. V-B), both based on the interval probability approximation $P_n^{(3)}$ in (29).

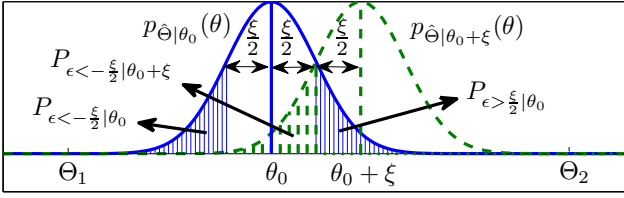


Figure 5. Decision problem with two equiprobable hypotheses: $H_1 : \Theta = \theta_0$ and $H_2 : \Theta = \theta_0 + \xi$.

A. An AUB

As $P_n^{(3)}$ approximates the probability that $\hat{\Theta}$ falls in D_n , the PDF of $\hat{\Theta}$ can be approximated by the limit of $P_n^{(3)}$ as N (number of intervals) approaches infinity (so that the width of D_n approaches zero). Accordingly we can write the approximate PDF, mean and MSE of $\hat{\Theta}$ as

$$p_M(\theta) = \lim_{N \rightarrow \infty} P_n^{(3)} = \frac{P(\theta, \Theta)}{\int_{\Theta_1}^{\Theta_2} P(\theta, \Theta) d\theta} \quad (55)$$

$$\mu_M = \int_{\Theta_1}^{\Theta_2} \theta p_M(\theta) d\theta \quad (56)$$

$$e_M = \int_{\Theta_1}^{\Theta_2} (\theta - \Theta)^2 p_M(\theta) d\theta. \quad (57)$$

We will see in Sec. VII that e_M acts as an UB and also converges to a multiple of the CRLB. In fact, $p_M(\theta)$ overestimates the true PDF of $\hat{\Theta}$ in the vicinity of Θ because it is obtained from $P_n^{(3)}$ which is in turn obtained from the interval probability UB $P_n^{(2)}$ in (27).

B. An MSEA

To guarantee the convergence of the MSEA to the CRLB, we approximate the PDF of $\hat{\Theta}$ inside $D_0 \approx [\Theta - \frac{\theta_1 - \Theta}{2}, \Theta + \frac{\theta_1 - \Theta}{2}]$ by $p_{0,N}(\theta)$ in (46) (Θ is the mean and $c(\Theta)$ is the MSE) and outside D_0 by $p'_M(\theta) = P(\theta, \Theta) / \int_{D_{\Theta} \setminus D_0} P(\theta, \Theta) d\theta$ (the corresponding mean and MSE are $\mu'_M = \int_{D_{\Theta} \setminus D_0} \theta p'_M(\theta) d\theta$ and $e'_M = \int_{D_{\Theta} \setminus D_0} (\theta - \Theta)^2 p'_M(\theta) d\theta$), and propose the following approximation:

$$p_{MN}(\theta) = (1 - \tilde{P}_A) p_{0,N}(\theta) + \tilde{P}_A p'_M(\theta) \quad (58)$$

$$\mu_{MN} = (1 - \tilde{P}_A) \Theta + \tilde{P}_A \mu'_M \quad (59)$$

$$e_{MN} = (1 - \tilde{P}_A) c(\Theta) + \tilde{P}_A e'_M \quad (60)$$

where $\tilde{P}_A = 2P(\theta_1, \Theta)$ approximates the probability that $\hat{\Theta}$ falls outside D_0 . With oscillating ACRs, θ_1 is the abscissa of the first local maximum after the global one; thus, $\theta_1 \approx \Theta + \frac{1}{f_c(\Theta)}$. With non-oscillating ACRs, the vicinity of the maximum is not clearly marked off; so, we empirically take $\theta_1 = \Theta + \frac{\pi}{4\beta_s(\Theta)}$.

The first contribution in this section is the AUB e_M which is very tight (as will be seen in Figs. 7 and 9) and also very easy to compute. The second one is the highly accurate MSEA e_{MN} (as will be seen in Figs. 6 and 8); to the best of our knowledge, this is the first approximation expressed as the sum of two terms when X_{n_1}, \dots, X_{n_N} are correlated (see [1, 15, 41, 43, 44]).

VI. ALBs

In this section we derive an ALB based on the Taylor series expansion of the noise limited to second order (Sec. VI-A) and a family of ALBs by employing the principle of binary detection which is first used by Ziv and Zakai [2] to derive LBs for Bayesian parameters (Sec. VI-B).

A. An ALB based on the second order Taylor series expansion of noise

From (33), the MLE of Θ can be approximated by:

$$\hat{\Theta} = \underset{\theta}{\operatorname{argmax}} \{X_{s,r}(\theta)\} \approx \hat{\Theta}_C = \Theta - \frac{\dot{w}_0}{\alpha \ddot{R}_0 + \ddot{w}_0} \quad (61)$$

where $\dot{w}_0/(\alpha \ddot{R}_0 + \ddot{w}_0)$ is a ratio of two normal variables. Statistics of normal variable ratios are studied in [57–59].

Let $\operatorname{sign}(\xi) = 1$ (resp. -1) for $\xi \geq 0$ (resp. $\xi < 0$), $\delta^4(\theta) = E_s(\theta)/E_s$, $h = \operatorname{sign}(\nu_0) \sigma_{\dot{w}_0} \sqrt{1 - \nu_0^2}$, $a_1 = \nu_0 \sigma_{\dot{w}_0} / \sigma_{\ddot{w}_0}$, $a_2 = \sigma_{\ddot{w}_0} / h$, $a_3 = \alpha \ddot{R}_0 a_1 / h$, $a_4 = -\alpha \ddot{R}_0 / \sigma_{\ddot{w}_0} = \sqrt{\rho} \beta^2(\Theta) / \delta^2(\Theta)$, $q(\xi) = (a_3 \xi + a_4) / \sqrt{1 + \xi^2}$. We can show from [58] that $\hat{\Theta}_C$ in (61) is distributed as:

$$\hat{\Theta}_C \sim \Theta + a_1 + \frac{\chi}{a_2} \quad (62)$$

where the PDF of χ is given by:

$$p_\chi(\xi) = \frac{e^{-\frac{a_3^2 + a_4^2}{2}}}{\pi(1 + \xi^2)} \left\{ 1 + \sqrt{2\pi} q(\xi) e^{\frac{q^2(\xi)}{2}} \left(\frac{1}{2} - Q[q(\xi)] \right) \right\}. \quad (63)$$

From (63) we can approximate the PDF, mean, variance and MSE of $\hat{\Theta}_C$ by

$$p_C(\theta) = \operatorname{sign}(\nu_0) a_2 p_\chi[a_2(\theta - \Theta - a_1)] \quad (64)$$

$$\mu_C = \int_{\Theta_1}^{\Theta_2} \theta p_C(\theta) d\theta \quad (65)$$

$$\sigma_C^2 = \int_{\Theta_1}^{\Theta_2} (\theta - \mu_C)^2 p_C(\theta) d\theta \quad (66)$$

$$e_C = (\mu_C - \Theta)^2 + \sigma_C^2. \quad (67)$$

Note that the moments $\int_{-\infty}^{\infty} \xi^i p_\chi(\xi) d\xi$, $i = 1, 2, \dots$ (infinite domain) are infinite like with Cauchy distribution [58]. We will see in Sec. VII that e_C behaves as an LB; this result can be expected from the approximation in (33) where the expansion of the noise is limited to second order.

B. Binary detection based ALBs

Let $\tilde{\Theta}$ be an estimator of Θ , $\epsilon|\theta = \tilde{\Theta} - \Theta$ the estimation error given $\Theta = \theta$, $p_{|\epsilon||\theta}(\xi)$ the PDF of $|\epsilon|$, and $P_{|\epsilon|>\xi|\theta}$ the probability that $|\epsilon| > \xi$. For $\Theta = \theta_0$, the MSE of $\tilde{\Theta}$ can be written as [60]:

$$\begin{aligned} e|\theta_0 &= \int_0^{\epsilon_{\max}} \xi^2 p_{|\epsilon||\theta_0}(\xi) d\xi = 2 \int_0^{\epsilon_{\max}} \xi P_{|\epsilon|>\xi|\theta_0} d\xi \\ &- \{\xi^2 P_{|\epsilon|>\xi|\theta_0}\} \Big|_0^{\epsilon_{\max}} = \frac{1}{2} \int_0^{2\epsilon_{\max}} \xi P_{|\epsilon|>\frac{\xi}{2}|\theta_0} d\xi \end{aligned} \quad (68)$$

where $\epsilon_{\max} = \max\{\Theta_2 - \theta_0, \theta_0 - \Theta_1\}$. By assuming $P_{\epsilon > \frac{\xi}{2}|\theta}$ and $P_{\epsilon < -\frac{\xi}{2}|\theta}$ constant $\forall \theta \in D_\Theta$, we can write ⁸:

$$P_{|\epsilon| > \frac{\xi}{2}|\theta_0} = 2 \left[\frac{1}{2} P_{\epsilon > \frac{\xi}{2}|\theta_0} + \frac{1}{2} P_{\epsilon < -\frac{\xi}{2}|\theta_0} \right] \quad (69)$$

$$\approx 2 \begin{cases} P_{\epsilon_1} = \frac{1}{2} P_{\epsilon > \frac{\xi}{2}|\theta_0 - \xi} + \frac{1}{2} P_{\epsilon < -\frac{\xi}{2}|\theta_0} \\ P_{\epsilon_2} = \frac{1}{2} P_{\epsilon > \frac{\xi}{2}|\theta_0} + \frac{1}{2} P_{\epsilon < -\frac{\xi}{2}|\theta_0 + \xi} \end{cases} \quad (70)$$

$$\geq 2 \begin{cases} P_{\min}(\theta_0 - \xi, \theta_0) \\ P_{\min}(\theta_0, \theta_0 + \xi) \end{cases}$$

where P_{ϵ_1} and P_{ϵ_2} denote the probabilities of error of the nearest decision rule

$$\hat{H} = \begin{cases} H_1 & \text{if } |\tilde{\Theta} - \{\Theta|H_1\}| \leq |\tilde{\Theta} - \{\Theta|H_2\}| \\ H_2 & \end{cases} \quad (71)$$

of the two-hypothesis decision problems (the decision problem in (73) is illustrated in Fig. 5):

$$H = \begin{cases} H_1 : \Theta = \theta_0 - \xi & P_{H_1} = 0.5 \\ H_2 : \Theta = \theta_0 & P_{H_2} = 0.5 \end{cases} \quad (72)$$

$$H = \begin{cases} H_1 : \Theta = \theta_0 & P_{H_1} = 0.5 \\ H_2 : \Theta = \theta_0 + \xi & P_{H_2} = 0.5 \end{cases} \quad (73)$$

and $P_{\min}(\theta_0 - \xi, \theta_0)$ and $P_{\min}(\theta_0, \theta_0 + \xi)$ the minimum probabilities of error obtained by the optimum decision rule based on the likelihood ratio test [36, pp. 30]:

$$\hat{H} = \begin{cases} H_1 & \text{if } \Lambda(\Theta|H_1) - \Lambda(\Theta|H_2) \geq \ln \frac{P_{H_2}}{P_{H_1}} \\ H_2 & \end{cases} \quad (74)$$

with $\Lambda(\theta)$ denoting the log-likelihood function in (2). The probability of error of an arbitrary detector \hat{H} is given by

$$P_e = P_{H_1} P_{\hat{H}=H_2|H_1} + P_{H_2} P_{\hat{H}=H_1|H_2}. \quad (75)$$

From (68) and (70) we obtain the following ALBs:

$$z_1 = \int_0^{\epsilon_1} \xi P_{\min}(\theta_0 - \xi, \theta_0) d\xi \quad (76)$$

$$z_2 = \int_0^{\epsilon_2} \xi P_{\min}(\theta_0, \theta_0 + \xi) d\xi \quad (77)$$

where $\epsilon_1 = \min\{\theta_0 - \Theta_1, 2(\Theta_2 - \theta_0)\}$ and $\epsilon_2 = \min\{\Theta_2 - \theta_0, 2(\theta_0 - \Theta_1)\}$. The integration limits are set to ϵ_1 and ϵ_2 to make the two hypotheses in (72) and (73) fall inside D_Θ . As $P_{|\epsilon| > \frac{\xi}{2}|\theta_0}$ is a decreasing function, tighter bounds can be obtained by filling the valleys of $P_{\min}(\theta_0 - \xi, \theta_0)$ and $P_{\min}(\theta_0, \theta_0 + \xi)$ (as proposed by Bellini and Tartara in [4]):

$$b_1 = \int_0^{\epsilon_1} \xi V\{P_{\min}(\theta_0 - \xi, \theta_0)\} d\xi \quad (78)$$

$$b_2 = \int_0^{\epsilon_2} \xi V\{P_{\min}(\theta_0, \theta_0 + \xi)\} d\xi \quad (79)$$

where $V\{f(\xi)\} = \max\{f(\zeta) \mid \zeta \geq \xi\}$ denotes the valley-filling function. When $P_{\min}(\theta, \theta')$ is a function of $\theta' - \theta$ (e.g, TOA estimation) we can write the bounds in (76)–(79) as ($i = 1, 2$):

$$z_i = \int_0^{\epsilon_i} \xi P_{\min}(\xi) d\xi \quad (80)$$

$$b_i = \int_0^{\epsilon_i} \xi V\{P_{\min}(\xi)\} d\xi. \quad (81)$$

⁸The obtained bounds are “approximate” due to this assumption; the assumption is valid when θ is not very close to the extremities of D_Θ .

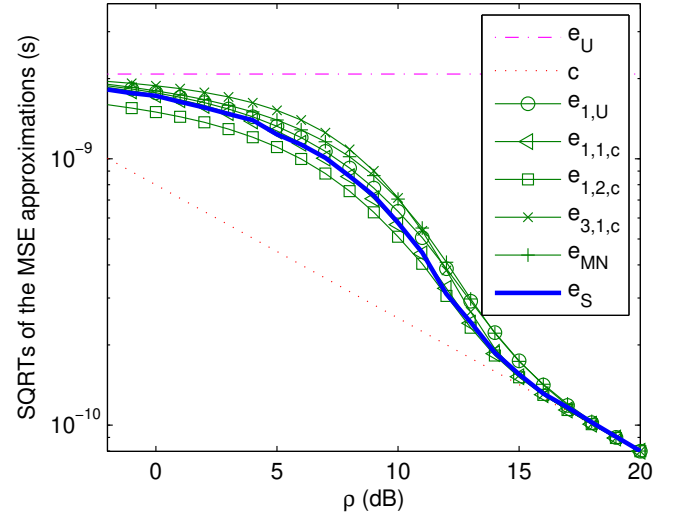


Figure 6. Baseband: SQRTs of the max. MSE e_U , the CRLB c , the MSEAs $e_{1,U}$, $e_{1,1,c}$, $e_{1,2,c}$, $e_{3,1,c}$ and e_{MN} , and the simulated MSE e_S , w.r.t. the SNR.

If $\theta_0 - \Theta_1 > \Theta_2 - \theta_0$, then $\epsilon_1 > \epsilon_2$; hence, z_1 and b_1 become tighter than z_2 and b_2 , respectively. From (2), (28), (74) and (75) we can write the minimum probability of error as

$$\begin{aligned} P_{\min}(\theta, \theta') &= 0.5 [P_{\Lambda(\theta') > \Lambda(\theta) | \Theta = \theta} + P_{\Lambda(\theta) > \Lambda(\theta') | \Theta = \theta'}] \\ &= 0.5 [P(\theta', \theta) |_{\Theta = \theta} + P(\theta, \theta') |_{\Theta = \theta'}] \\ &= Q \left(\sqrt{\frac{\rho}{2}} [1 - R(\theta, \theta')] \right). \end{aligned} \quad (82)$$

There are two main differences between our bounds (deterministic) and the Bayesian ones: i) with the former we integrate along the error only whereas with the latter we integrate along the error and the *a priori* distribution of Θ (e.g, see (14) in [21]); ii) all hypotheses (e.g, $\Theta = \theta_0$ and $\Theta = \theta_0 + \xi$ in (73)) are possible in the Bayesian case thanks to the *a priori* distribution whereas only one hypothesis ($\Theta = \theta_0$) is possible in the deterministic case. So in order to utilize the minimum probability of error we have approximated $P_{\epsilon < -\frac{\xi}{2}|\theta_0}$ in (69) by $P_{\epsilon < -\frac{\xi}{2}|\theta_0 + \xi}$ (see Fig. (5)).

In this section we have two main contributions. The first one is the ALB e_C whereas the second one is the deterministic ZZLB family. These bounds can from now on be used as benchmarks in deterministic parameter estimation (like the CRLB) where it is not rigorous to use Bayesian bounds. Even though the derivation of e_C was a bit complex, the final expression is now ready to be utilized.

VII. NUMERICAL RESULTS AND DISCUSSION

In this section we discuss some numerical results about the derived MSEAs, AUB, and ALBs. We consider TOA estimation using baseband and passband pulses. Let $T_w = 2$ ns, $f_c = 6.85$ GHz, $\Theta = 0$ and $D_\Theta = [-2, 1.5]T_w$. With the baseband pulse we consider 9 equal duration intervals. Let

$$e_{i,j,x} = P_0^{(i)} \sigma_{0,0}^2 + \sum_{n=n_1, n \neq 0}^{n_N} P_n^{(i)} [(\Theta - \mu_{n,j,x})^2 + \sigma_{n,j,x}^2] \quad (83)$$

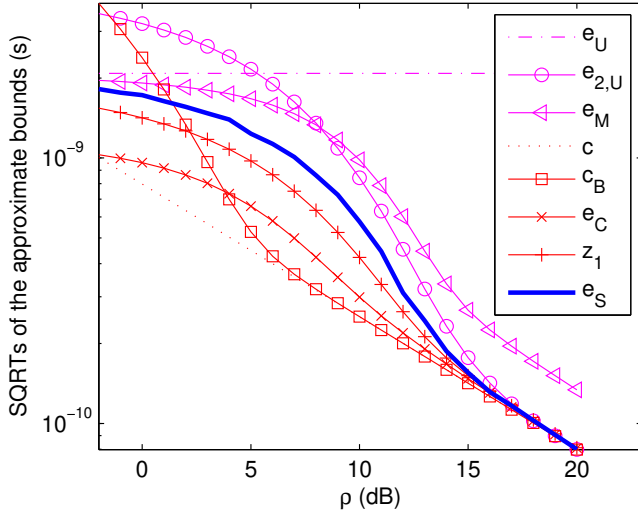


Figure 7. Baseband: SQRTs of the max. MSE e_U , the AUBs $e_{2,U}$ and e_M , the CRLB c , the BLB c_B , the ALBs e_C and z_1 , and the simulated MSE e_S , w.r.t. the SNR.

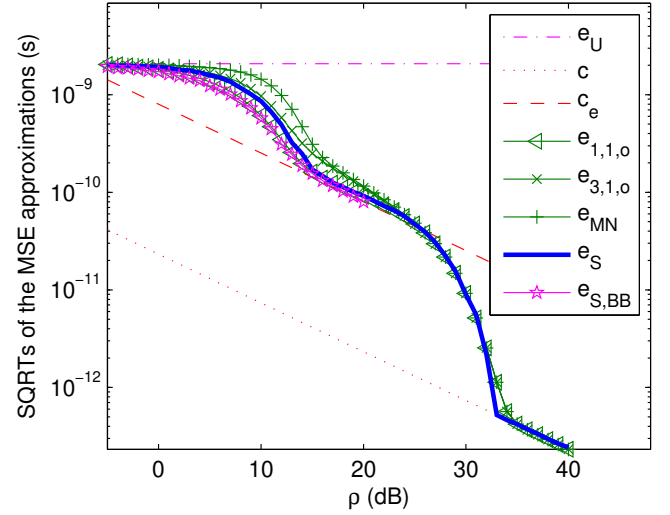


Figure 8. Passband: SQRTs of the max. MSE e_U , the CRLB c , the ECRLB c_e , the MSEAs $e_{1,1,o}$, $e_{3,1,o}$ and e_{MN} , and the simulated MSEs of the passband e_S and baseband $e_{S,BB}$ pulses, w.r.t. the SNR.

be the MSEA based on (22) and using the interval probability approximation $P_n^{(i)}$ ($i \in \{1, 2, 3\}$, see (26), (27), (29)) and interval mean and variance approximations $\mu_{n,j,x}$ and $\sigma_{n,j,x}^2$ ($(j, x) = U$ in (30), (31), and $(j, x) \in \{1, 2\} \times \{c, o\}$ in (41)–(44), (49)–(52)).

A. Baseband pulse

Consider first the baseband pulse. In Fig. 6 we show the SQRTs of the maximum MSE e_U in (19), the CRLB c in (8), five MSEAs: $e_{1,U}$, $e_{1,1,c}$, $e_{1,2,c}$, $e_{3,1,c}$ in (83) and e_{MN} in (60), and the MSE e_S obtained by simulation based on 10000 trials, versus the SNR. In Fig. 7 we show the SQRTs of e_U , two AUBs: $e_{2,U}$ in (83) and e_M in (57), c , the BLB c_B in (18), two ALBs: e_C in (67) and z_1 in (80) (equal to b_1 in (81) because a non-oscillating ACR), and e_S .

We can see from e_S that, as cleared up in Sec. I, the SNR axis can be divided into three regions: 1) the *a priori* region where e_U is achieved, 2) the threshold region and 3) the asymptotic region where c is achieved. We define the *a priori* and asymptotic thresholds by [7]:

$$\rho_{pr} = \rho : e(\rho) = \alpha_{pr} e_U \quad (84)$$

$$\rho_{as} = \rho : e(\rho) = \alpha_{as} c. \quad (85)$$

We take $\alpha_{pr} = 0.5$ and $\alpha_{pr} = 1.1$. From e_S , we have $\rho_{pr} = 4$ dB and $\rho_{as} = 16$ dB. Thresholds are defined in literature w.r.t. two magnitudes at least: i) the achieved MSE [7, 9, 21] like in our case (which is the most reliable because the main concern in estimation is to minimize the MSE) and ii) the probability of non-ambiguity [15, 37] (for simplicity reasons).

The MSEAs $e_{1,U}$, $e_{1,1,c}$, $e_{1,2,c}$, $e_{3,1,c}$ obtained from the MIE (Sec. IV) are very accurate and follow e_S closely; $e_{1,1,c}$ is more accurate than $e_{3,1,c}$ which slightly overestimates e_S because $e_{1,1,c}$ uses the probability approximation $P_n^{(1)}$ in (26) that considers all testpoints during the computation of the probability, whereas $e_{3,1,c}$ uses the approximation $P_n^{(3)}$ in (29)

based on the probability UB $P_n^{(2)}$ in (27) that only considers the 0th and the n th testpoints; $e_{1,1,c}$ is more accurate than $e_{1,U}$ which slightly overestimates e_S , and than $e_{1,2,c}$ which slightly underestimates it, because $e_{1,1,c}$ uses the variance approximation $\sigma_{n,1,c}^2$ in (42) obtained from the first order Taylor series expansion of noise, whereas $e_{1,U}$ uses $\sigma_{n,U}^2$ in (31) assuming the MLE uniformly distributed in D_n (overestimation of the noise), and $e_{1,2,c}$ uses $\sigma_{n,2,c}^2$ in (44) neglecting the noise. The MSEA e_{MN} proposed in Sec. V-A based on our probability approximation $P_n^{(3)}$ is very accurate as well.

The AUB $e_{2,U}$ proposed in [1] is very tight and converges to the asymptotic region simultaneously with e_S . However, it is less tight in the *a priori* and threshold regions because it uses the probability UB $P_n^{(2)}$ which is not very tight in these regions (see Fig. 3). Moreover, $e_{2,U} \rightarrow \infty$ when $N \rightarrow \infty$. The AUB e_M (Sec. V-A) is very tight. However, it converges to 2.68 times the CRLB at high SNRs. This fact was discussed in Sec. V-A and also solved in Sec. V-B by proposing e_{MN} (examined above). Nevertheless, e_M can be used to compute the asymptotic threshold accurately because it converges to its own asymptotic regime simultaneously with e_S .

Both the BLB c_B and the ALB e_C (Sec. VI-A) outperform the CRLB. Unlike the passband case considered below, e_C outperforms the BLB. The ALB z_1 (Sec. VI-B) is very tight and converges to the CRLB simultaneously with e_S .

B. Passband pulse

Consider now the passband pulse. In Fig. 8 we show the SQRTs of the maximum MSE e_U , the CRLB c , the ECRLB c_e in (15) (equal to CRLB of the baseband pulse), three MSEAs: $e_{1,1,o}$ and $e_{3,1,o}$ in (83) and e_{MN} in (60), and the MSEs obtained by simulation for both the passband e_S and the baseband $e_{S,BB}$ pulses. In Fig. 9 we show the SQRTs of e_U , two AUBs: $e_{2,U}$ in (83) and e_M in (57), c , c_e , the BLB c_B , three ALBs: e_C in (67), z_1 in (80) and b_1 in (81), and e_S .

By observing e_S , we identify five regions: 1) the *a priori* region, 2) the *a priori*-ambiguity transition region, 3) the ambiguity region where the ECRLB is achieved, 4) the ambiguity-asymptotic transition region and 5) the asymptotic region. We define the begin-ambiguity and end-ambiguity thresholds marking the ambiguity region by [7]

$$\rho_{am1} = \rho : e(\rho) = \alpha_{am1} c_e \quad (86)$$

$$\rho_{am2} = \rho : e(\rho) = \alpha_{am2} c_e. \quad (87)$$

We take $\alpha_{am1} = 2$ and $\alpha_{am2} = 0.5$. From e_S we have $\rho_{pr} = 7$ dB, $\rho_{am1} = 15$ dB, $\rho_{am2} = 28$ dB and $\rho_{as} = 33$ dB.

The MSEAs $e_{1,1,o}$, $e_{3,1,o}$ (Sec. IV) and e_{MN} (Sec. V-B) are highly accurate and follow e_S closely.

The AUB $e_{2,U}$ [1] is very tight beyond the *a priori* region. The AUB e_M (Sec. V-A) is very tight. However, it converges to 1.75 times the CRLB in the asymptotic region.

The BLB c_B detects the ambiguity and asymptotic regions much below the true ones; consequently, it does not determine accurately the thresholds ($\rho_{am1} = 5$ dB, $\rho_{am2} = 20$ dB and $\rho_{as} = 26$ dB instead of 15, 28 and 33 dB). The ALB e_C (Sec. VI-A) outperforms the CRLB, but is outperformed by the BLB (unlike the baseband case). The ALB z_1 (Sec. VI-B) is very tight, but b_1 (Sec. VI-B) is tighter thanks to the valley-filling function. They both can calculate accurately the asymptotic threshold and to detect roughly the ambiguity region.

Let us compare the MSEs $e_{S,BB}$ and e_S achieved by the baseband and passband pulses (Fig. 8). Both pulses approximately achieve the same MSE below the end-ambiguity threshold of the passband pulse ($\rho_{am2} = 28$ dB) and achieve the ECRLB between the begin-ambiguity and end-ambiguity thresholds. The MSE achieved with the baseband pulse is slightly smaller than that achieved with the passband pulse because with the former the estimates spread in continuous manner along the ACR whereas with the latter they spread around the local maxima. The asymptotic threshold of the baseband pulse (16 dB) is approximately equal to the begin-ambiguity threshold of the passband pulse (15 dB). Above the end-ambiguity threshold, the MSE of the passband pulse rapidly converges to the CRLB while that of the baseband one remains equal to the ECRLB.

To summarize we can say that for a given nonlinear estimation problem with an oscillating ACR, the MSE achieved by the ACR below the end-ambiguity threshold is the same as that achieved by its envelope. Between the begin-ambiguity and end-ambiguity thresholds, the achieved MSE is equal to the ECRLB. Above the latter threshold, the MSE achieved by the ACR converges to the CRLB whereas that achieved by its envelope remains equal to the ECRLB.

VIII. CONCLUSION

We have considered nonlinear estimation of scalar deterministic parameters and investigated the threshold and ambiguity phenomena. The MIE is employed to approximate the statistics of the MLE. The obtained MSEAs are highly accurate and follow the true MSE closely. A very tight AUB is proposed as well. An ALB tighter than the CRLB is derived using the

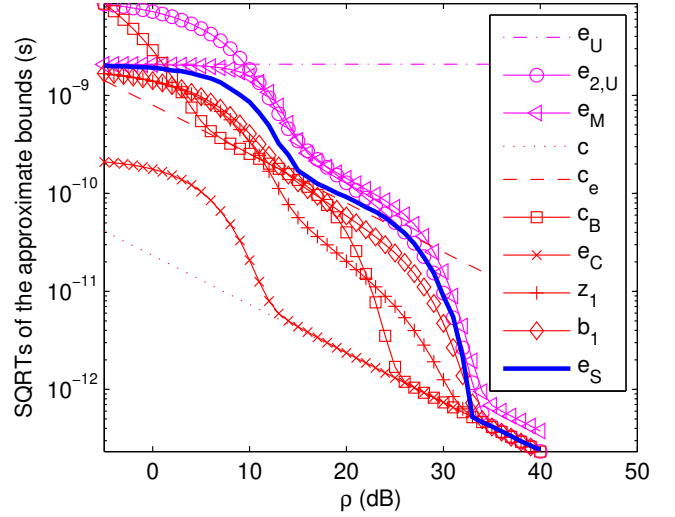


Figure 9. Passband: SQRTs of the max. MSE e_U , the AUBs $e_{2,U}$ and e_M , the CRLB c , the ECRLB c_e , the BLB c_B , the ALBs e_C , z_1 and b_1 , and the simulated MSE e_S , w.r.t. the SNR.

second order Taylor series expansion of noise. The principle of binary detection is utilized to compute some ALBs which are very tight.

APPENDIX A

CURVATURES OF THE ACR AND OF ITS ENVELOPE

In this appendix we prove (14). From (11) and (13) we can write the FT of the complex envelope $e_{R_s}(\theta, \Theta)$ as

$$\mathcal{F}_{e_{R_s}}(f) = 2\mathcal{F}_{R_s}^+[f + f_c(\Theta)] \quad (88)$$

where $x^+(f) = \begin{cases} x(f) & f > 0 \\ 0 & f \leq 0 \end{cases}$. From (13) we can write

$$\ddot{R}_s(\theta, \Theta) = \Re \left\{ e^{j2\pi(\theta-\Theta)f_c(\Theta)} [j4\pi f_c(\Theta) \dot{e}_{R_s}(\theta, \Theta) + \ddot{e}_{R_s}(\theta, \Theta) - 4\pi^2 f_c^2(\Theta) e_{R_s}(\theta, \Theta)] \right\} \quad (89)$$

As from (13) $\Re\{e_{R_s}(\Theta, \Theta)\} = R_s(\Theta, \Theta) = E_s$, (89) gives

$$\ddot{R}_s(\Theta, \Theta) = \Re\{\ddot{e}_{R_s}(\Theta, \Theta)\} - 4\pi^2 f_c^2(\Theta) E_s + 4\pi f_c(\Theta) \Re\{j\dot{e}_{R_s}(\Theta, \Theta)\}. \quad (90)$$

To prove (14) from (90) we must prove that $\Re\{j\dot{e}_{R_s}(\Theta, \Theta)\}$ is null. Using (88) and the inverse FT, we can write

$$\begin{aligned} \dot{e}_{R_s}(\theta, \Theta) &= \int_{-\infty}^{+\infty} j2\pi f \mathcal{F}_{e_{R_s}}(f) e^{j2\pi f(\theta-\Theta)} df \\ &= \int_{-\infty}^{+\infty} j4\pi f \mathcal{F}_{R_s}^+[f + f_c(\Theta)] e^{j2\pi f(\theta-\Theta)} df \\ &= \int_{-\infty}^{+\infty} j4\pi [f - f_c(\Theta)] \mathcal{F}_{R_s}^+(f) e^{j2\pi [f - f_c(\Theta)](\theta-\Theta)} df \\ &= \int_0^{+\infty} j4\pi [f - f_c(\Theta)] \mathcal{F}_{R_s}(f) e^{j2\pi [f - f_c(\Theta)](\theta-\Theta)} df \end{aligned}$$

so $\dot{e}_{R_s}(\Theta, \Theta) = \int_0^{+\infty} j4\pi [f - f_c(\Theta)] \mathcal{F}_{R_s}(f) df$. Using (12) and the last equation, $\Re\{j\dot{e}_{R_s}(\Theta, \Theta)\}$ becomes

$$\Re\{j\dot{e}_{R_s}(\Theta, \Theta)\} = - \int_0^{+\infty} 4\pi [f - f_c(\Theta)] \Re\{\mathcal{F}_{R_s}(f)\} df = 0.$$

Hence, (14) is proved.

ACKNOWLEDGMENT

The authors would like to thank Prof. Alan Genz for his help in the probability numerical computation.

REFERENCES

- [1] R. McAulay and D. Sakrison, "A PPM/PM hybrid modulation system," *IEEE Trans. Commun. Technol.*, vol. 17, no. 4, pp. 458–469, Aug. 1969.
- [2] J. Ziv and M. Zakai, "Some lower bounds on signal parameter estimation," *IEEE Trans. Inf. Theory*, vol. 15, no. 3, pp. 386–391, May 1969.
- [3] L. Seidman, "Performance limitations and error calculations for parameter estimation," *Proc. IEEE*, vol. 58, no. 5, pp. 644–652, May 1970.
- [4] S. Bellini and G. Tartara, "Bounds on error in signal parameter estimation," *IEEE Trans. Commun.*, vol. 22, no. 3, pp. 340–342, Mar. 1974.
- [5] S.-K. Chow and P. Schultheiss, "Delay estimation using narrow-band processes," *IEEE Trans. Acoust., Speech, Signal Process.*, vol. 29, no. 3, pp. 478–484, June 1981.
- [6] A. Weiss and E. Weinstein, "Fundamental limitations in passive time delay estimation—part I: Narrow-band systems," *IEEE Trans. Acoust., Speech, Signal Process.*, vol. 31, no. 2, pp. 472–486, Apr. 1983.
- [7] E. Weinstein and A. Weiss, "Fundamental limitations in passive time delay estimation—part II: Wide-band systems," *IEEE Trans. Acoust., Speech, Signal Process.*, vol. 32, no. 5, pp. 1064–1078, Oct. 1984.
- [8] A. Zeira and P. Schultheiss, "Realizable lower bounds for time delay estimation," *IEEE Trans. Signal Process.*, vol. 41, no. 11, pp. 3102–3113, Nov. 1993.
- [9] —, "Realizable lower bounds for time delay estimation. 2. threshold phenomena," *IEEE Trans. Signal Process.*, vol. 42, no. 5, pp. 1001–1007, May 1994.
- [10] B. Sadler and R. Kozick, "A survey of time delay estimation performance bounds," in *4th IEEE Workshop Sensor Array, Multichannel Process.*, July 2006, pp. 282–288.
- [11] B. Sadler, L. Huang, and Z. Xu, "Ziv-Zakai time delay estimation bound for ultra-wideband signals," in *IEEE Int. Conf. Acoust., Speech, Signal Process. (ICASSP 2007)*, vol. 3, Apr. 2007, pp. III–549–III–552.
- [12] S. Zafer, S. Gezici, and I. Guvenc, *Ultra-wideband Positioning Systems: Theoretical Limits, Ranging Algorithms, and Protocols*. Cambridge University Press, 2008.
- [13] A. Renaux, P. Forster, E. Chaumette, and P. Larzabal, "On the high-snr conditional maximum-likelihood estimator full statistical characterization," *IEEE Trans. Signal Process.*, vol. 54, no. 12, pp. 4840–4843, Dec. 2006.
- [14] A. Renaux, P. Forster, E. Boyer, and P. Larzabal, "Unconditional maximum likelihood performance at finite number of samples and high signal-to-noise ratio," *IEEE Trans. Signal Process.*, vol. 55, no. 5, pp. 2358–2364, May 2007.
- [15] C. Richmond, "Capon algorithm mean-squared error threshold snr prediction and probability of resolution," *IEEE Trans. Signal Process.*, vol. 53, no. 8, pp. 2748–2764, Aug. 2005.
- [16] A. Renaux, "Contribution à l'analyse des performances d'estimation en traitement statistique du signal," Ph.D. dissertation, ENS CACHAN, 2006.
- [17] L. Seidman, "An upper bound on average estimation error in nonlinear systems," *IEEE Trans. Inf. Theory*, vol. 14, no. 2, pp. 243–250, Mar. 1968.
- [18] H. L. Van Trees and K. L. Bell, Eds., *Bayesian Bounds for Parameter Estimation and Nonlinear Filtering/Tracking*. Wiley-IEEE Press, 2007.
- [19] D. Chazan, M. Zakai, and J. Ziv, "Improved lower bounds on signal parameter estimation," *IEEE Trans. Inf. Theory*, vol. 21, no. 1, pp. 90–93, Jan. 1975.
- [20] E. Weinstein, "Relations between Bellini-Tartara, Chazan-Zakai-Ziv, and Wax-Ziv lower bounds," *IEEE Trans. Inf. Theory*, vol. 34, no. 2, pp. 342–343, Mar. 1988.
- [21] K. Bell, Y. Steinberg, Y. Ephraim, and H. Van Trees, "Extended Ziv-Zakai lower bound for vector parameter estimation," *IEEE Trans. Inf. Theory*, vol. 43, no. 2, pp. 624–637, Mar. 1997.
- [22] I. Reuven and H. Messer, "A Barankin-type lower bound on the estimation error of a hybrid parameter vector," *IEEE Trans. Inf. Theory*, vol. 43, no. 3, pp. 1084–1093, May 1997.
- [23] S. Kay, *Fundamentals of Statistical Signal Processing Estimation Theory*. Prentice-Hall, 1993.
- [24] E. W. Barankin, "Locally best unbiased estimators," *Ann. Math. Statist.*, vol. 20, pp. 477–501, Dec. 1949.
- [25] R. McAulay and L. Seidman, "A useful form of the Barankin lower bound and its application to PPM threshold analysis," *IEEE Trans. Inf. Theory*, vol. 15, no. 2, pp. 273–279, Mar. 1969.
- [26] R. McAulay and E. Hofstetter, "Barankin bounds on parameter estimation," *IEEE Trans. Inf. Theory*, vol. 17, no. 6, pp. 669–676, Nov. 1971.
- [27] P. Swerling, "Parameter estimation for waveforms in additive Gaussian noise," *J. Soc. Ind. Appl. Math.*, vol. 7, no. 2, pp. 152–166, June 1959.
- [28] L. Knockaert, "The Barankin bound and threshold behavior in frequency estimation," *IEEE Trans. Signal Process.*, vol. 45, no. 9, pp. 2398–2401, Sept. 1997.
- [29] L. Seidman, "The performance of a PPM/PM hybrid modulation system," *IEEE Trans. Commun. Technol.*, vol. 18, no. 5, pp. 697–698, Oct. 1970.
- [30] D. Dardari, C.-C. Chong, and M. Win, "Improved lower bounds on time-of-arrival estimation error in realistic UWB channels," in *2006 IEEE Int. Conf. Ultra-Wideband (ICUWB 2006)*, Sept. 2006, pp. 531–537.
- [31] B. Sadler, L. Huang, and Z. Xu, "Ziv-Zakai time delay estimation bound for ultra-wideband signals," in *IEEE Int. Conf. Acoust., Speech, Signal Process. (ICASSP 2007)*, vol. 3, Apr. 2007, pp. III–549–III–552.
- [32] R. Kozick and B. Sadler, "Bounds and algorithms for time delay estimation on parallel, flat fading channels," in *IEEE Int. Conf. Acoust., Speech, Signal Process. (ICASSP 2008)*, Apr. 2008, pp. 2413–2416.
- [33] D. Dardari, C.-C. Chong, and M. Win, "Threshold-based time-of-arrival estimators in UWB dense multipath channels," *IEEE Trans. Commun.*, vol. 56, no. 8, pp. 1366–1378, Aug. 2008.
- [34] D. Dardari, A. Conti, U. Finner, A. Giorgetti, and M. Win, "Ranging with ultrawide bandwidth signals in multipath environments," *Proc. IEEE*, vol. 97, no. 2, pp. 404–426, Feb. 2009.
- [35] D. Dardari and M. Win, "Ziv-Zakai bound on time-of-arrival estimation with statistical channel knowledge at the receiver," in *IEEE Int. Conf. Ultra-Wideband (ICUWB 2009)*, Sept. 2009, pp. 624–629.
- [36] J. M. Wozencraft and I. M. Jacobs, *Principles of Communication Engineering*. Wiley, 1965.
- [37] H. L. Van Trees, *Detection, Estimation, and Modulation Theory, Part I*. Wiley, 1968.
- [38] P. M. Woodward, *Probability and Information Theory With Applications To Radar*. McGraw-Hill, 1955.
- [39] V. A. Kotelnikov, *The Theory of Optimum Noise Immunity*. McGraw-Hill, 1959.
- [40] D. Rife and R. Boorstyn, "Single tone parameter estimation from discrete-time observations," *IEEE Trans. Inf. Theory*, vol. 20, no. 5, pp. 591–598, Sept. 1974.
- [41] L. Najjar-Atallah, P. Larzabal, and P. Forster, "Threshold region determination of ml estimation in known phase data-aided frequency synchronization," *IEEE Signal Process. Lett.*, vol. 12, no. 9, pp. 605–608, Sept. 2005.
- [42] E. Boyer, P. Forster, and P. Larzabal, "Nonasymptotic statistical performance of beamforming for deterministic signals," *IEEE Signal Process. Lett.*, vol. 11, no. 1, pp. 20–22, Jan. 2004.
- [43] F. Athley, "Threshold region performance of maximum likelihood direction of arrival estimators," *IEEE Trans. Signal Process.*, vol. 53, no. 4, pp. 1359–1373, Apr. 2005.
- [44] C. Richmond, "Mean-squared error and threshold snr prediction of maximum-likelihood signal parameter estimation with estimated colored noise covariances," *IEEE Trans. Inf. Theory*, vol. 52, no. 5, pp. 2146–2164, May 2006.
- [45] A. Mallat, S. Gezici, D. Dardari, C. Craeye, and L. Vandendorpe, "Statistics of the MLE and approximate upper and lower bounds – part 1: Application to TOA estimation," *Under submission*.
- [46] A. Mallat, S. Gezici, D. Dardari, and L. Vandendorpe, "Statistics of the MLE and approximate upper and lower bounds – part 2: Threshold computation and optimal signal design," *Under submission*.
- [47] A. Mallat, J. Louveaux, and L. Vandendorpe, "UWB based positioning in multipath channels: CRBs for AOA and for hybrid TOA-AOA based methods," in *IEEE Int. Conf. Commun. (ICC 2007)*, June 2007, pp. 5775–5780.
- [48] M. I. Skolnik, Ed., *Radar Handbook*. McGraw-Hill, 1970.
- [49] Federal Communications Commission (FCC), "Revision of part 15 of the commission rules regarding ultra-wideband transmission systems," in *FCC 02-48*, Apr. 2002.
- [50] A. Mallat, P. Gerard, M. Drouguet, F. Keshmiri, C. Oestges, C. Craeye, D. Flandre, and L. Vandendorpe, "Testbed for IR-UWB based ranging and positioning: Experimental performance and comparison to CRLBs," in *5th IEEE Int. Symp. Wireless Pervasive Comput. (ISWPC 2010)*, May 2010, pp. 163–168.
- [51] A. Genz, "Numerical computation of multivariate normal probabilities," *J. Comp. Graph. Stat.*, vol. 1, no. 2, pp. 141–149, June 1992.

- [52] —, “On a number-theoretical integration method,” *Aequationes Mathematicae*, vol. 8, no. 3, pp. 304–311, Oct. 1972.
- [53] —, “Randomization of number theoretic methods for multiple integration,” *SIAM J. Numer. Anal.*, vol. 13, no. 6, pp. 904–914, Dec. 1976.
- [54] D. Nuyens and R. Cools, “Fast component-by-component construction, a reprise for different kernels,” *H. Niederreiter and D. Talay editors, Monte-Carlo and Quasi-Monte Carlo Methods*, pp. 371–385, 2004.
- [55] H. I. Jacobson, “The maximum variance of restricted unimodal distributions,” *Ann. Math. Statist.*, vol. 40, no. 5, pp. 1746–1752, Oct. 1969.
- [56] S. W. Dharmadhikari and K. Joag-Dev, “Upper bounds for the variances of certain random variables,” *Commun. Stat. Theor. M.*, vol. 18, no. 9, pp. 3235–3247, 1989.
- [57] G. Marsaglia, “Ratios of normal variables and ratios of sums of uniform variables,” *J. Amer. Statist. Assoc.*, vol. 60, no. 309, pp. 193–204, Mar. 1965.
- [58] —, “Ratios of normal variables,” *J. Stat. Softw.*, vol. 16, no. 4, May 2006.
- [59] D. V. Hinkley, “On the ratio of two correlated normal random variable,” *Biometrika*, vol. 56, no. 3, pp. 635–639, Dec. 1969.
- [60] E. Cinlar, *Introduction to Stochastic Process*. Englewood Cliffs, NJ: Prentice Hall, 1975.